Electronic Supplementary Material (ESI) for Journal of Materials Chemistry A.

In this supplementary section, we provide additional structural and transport data to increase the transparency of the results presented within the main body. All X-ray diffraction traces are shown (Figure S1 and S2). The total thermal conductivity is provided in Figure S3, as the lattice thermal conductivity in main body requires subtraction of the electronic component of thermal conductivity. Finally, the zT for each sample is calculated and presented in Figure S4.

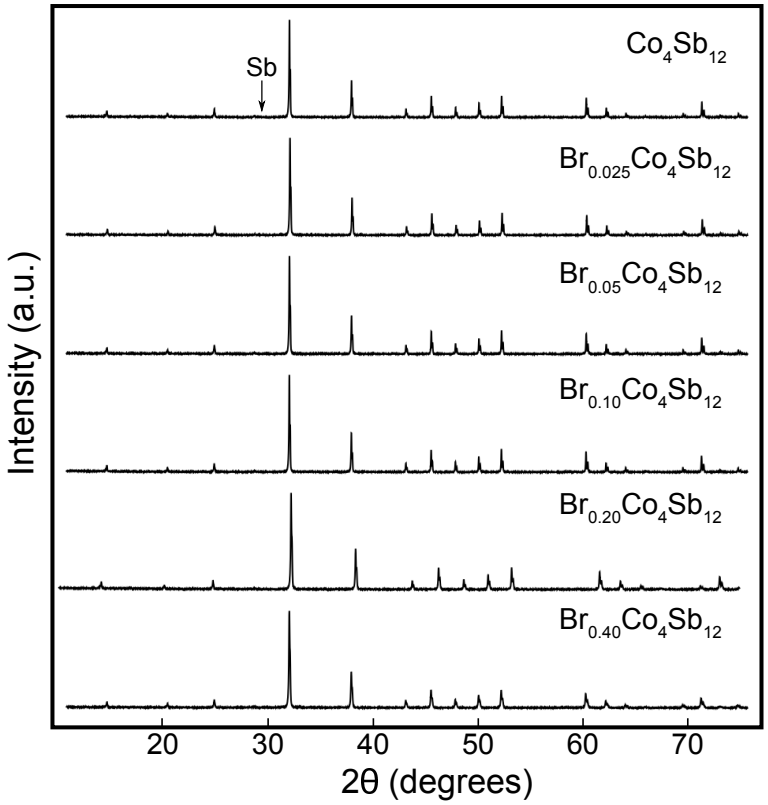

Figure S1 XRD patterns collected on samples of $Br_xCo_4Sb_{12}$ used in the initial crystallographic study show the material is largely phase pure $CoSb_3$ with a ($<$2 at.%) impurity of elemental antimony. Antimony peaks are too small to be resolved on the figure, but can be refined via Rietveld refinement. Changes in lattice parameter are subtle, and not able to be resolved via inspection.

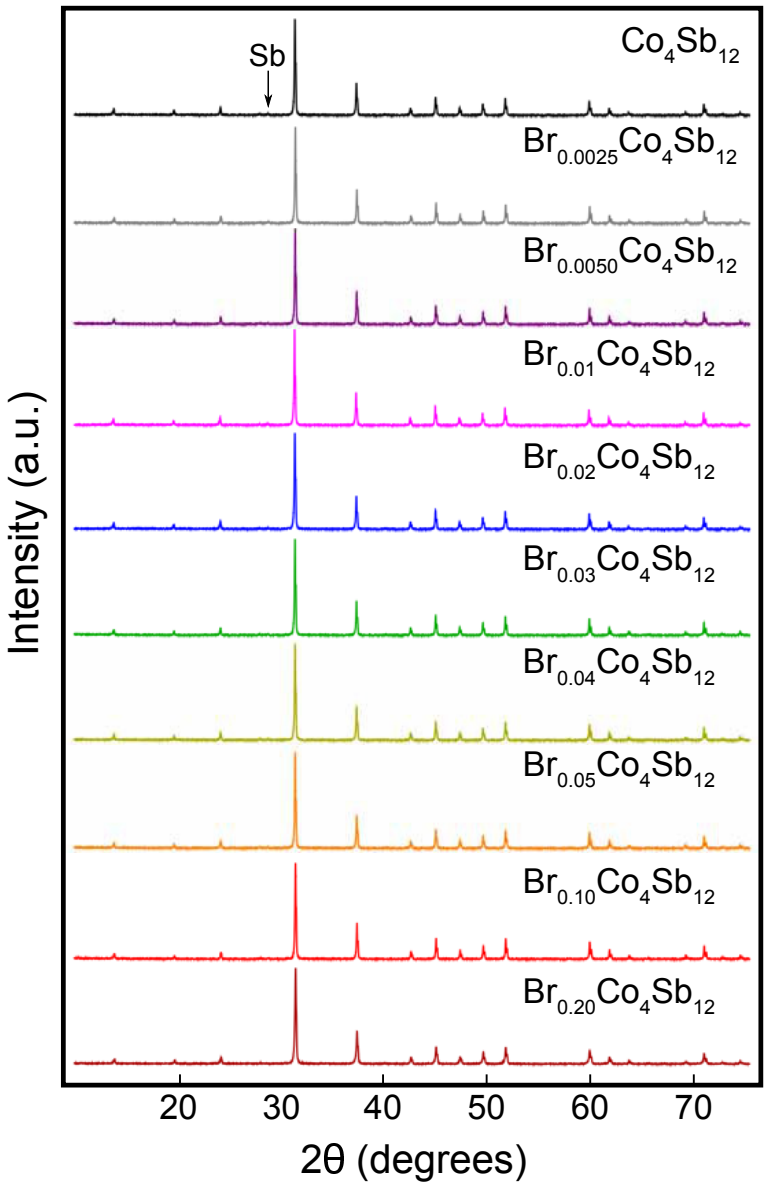

Figure S2 XRD patterns collected on sintered samples of $Br_xCo_4Sb_{12}$ used for electronic transport, thermal transport, and XRF results show the material is largely phase pure $CoSb_3$ with a (<2 at.%) impurity of elemental antimony. Antimony peaks are too small to be resolved on the figure, but can be refined via Rietveld refinement.

Table S1 Rietveld results for samples shown in Figure 2 inset. Lattice parameter, isotropic domain size, and the atomic positions of Co and Sb were explicitly refined. The base structure for refinement was pure $CoSb_3$ (ICSD: 62110) and did not include Br atoms. All atomic occupancies were set to 1.00 and were not refined. Thermal parameters were set to 0.01 for all atoms and were not refined. Note that the isotropic domain size was used as the primary experimental broadening parameter within the refinement. Microstrain was neither refined nor included in the refinement. We acknowledge that different combinations of microstrain and domain size could be used and achieve fits with comparable chi-squared for lab XRD data; accordingly, we do not try to extract any information from the domain size. Also shown is the resulting reduced chi-squared for each fit.

Sample	a (Å)	domain (μm)	X_{Co}	X_{Sb}	χ^2
Co_4Sb_{12}	9.03513	0.19057	(0, 0, 0)	(0,0.33385,0.15755)	1.90
$Br_{0.025}Co_4Sb_{12}$	9.03629	0.16963	(0, 0, 0)	(0, 0.33388, 0.15780)	1.88
$Br_{0.050}Co_4Sb_{12}$	9.03794	0.17478	(0, 0, 0)	(0, 0.33363, 0.15717)	1.76
$Br_{0.100}Co_4Sb_{12}$	9.03987	0.18146	(0, 0, 0)	(0, 0.33425, 0.15790)	1.80
$Br_{0.200}Co_4Sb_{12}$	9.04235	0.13599	(0, 0, 0)	(0, 0.33411, 0.15723)	1.57
$Br_{0.400}Co_4Sb_{12}$	9.04463	0.11650	(0, 0, 0)	(0, 0.33340, 0.15752)	1.91

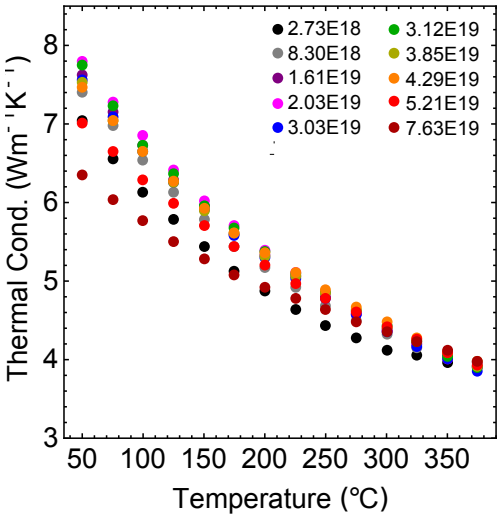

Figure S3 Total thermal conductivity collected on samples of $Br_xCo_4Sb_{12}$. Changes in total thermal conductivity do not track monotonically with increases in bromine concentration due to changes in the electronic contribution to thermal conductivity.

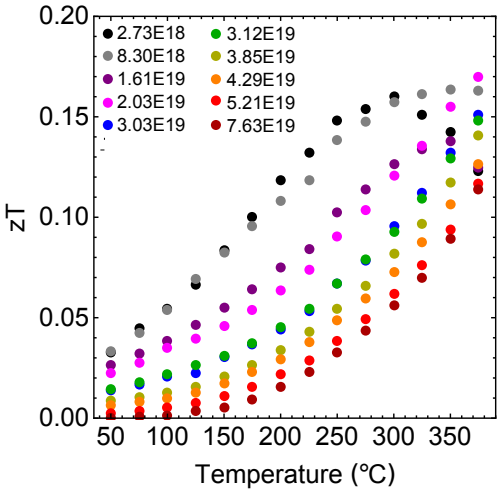

Figure S4 Combining high temperature transport results allows calculation of zT. Due to a conservative maximum temperature, and a relatively low filling fraction compared to optimally doped *p*-type skutterudite, values of zT are approximately half that of fully optimized skutterudite at similar temperatures.